Renewable Energy 145 (2020) 428–441

Contents lists available at ScienceDirect

Renewable Energy

journal homepage: www.elsevier.com/locate/renene

Performance improvement of a flat-plate solar collector by inserting intermittent porous blocks

K. Anirudh, S. Dhinakaran*

The Centre for Fluid Dynamics, Discipline of Mechanical Engineering, Indian Institute of Technology Indore, Simrol, Indore, 453 552, India

ARTICLE INFO

Article history:
Received 28 February 2019
Received in revised form
13 May 2019
Accepted 4 June 2019
Available online 7 June 2019

Keywords:
Flat-plate solar collector
Porous blocks
Performance enhancement
Darcy-Brinkman-Forchheimer model

ABSTRACT

Numerical analysis of the thermal performance of a flat plate solar collector (FPSC) is presented. The FPSC is inserted with porous metal foam blocks intermittently for promoting thermal mixing. Based on the presence of blocks at the inlet and the outlet, four different arrangements are used namely NN, NP, PN and PP, wherein N means absent, and P means present. Also, four different cases based on the increasing number of porous blocks as per respective arrangement are considered viz., Case 1 with 1 or 2, Case 2 with 3 or 4, Case 3 with 5 or 6, and Case 4 with 7 or 8 porous blocks. Influence of height of porous blocks ($S = 0–1$), and permeability of the porous medium (Darcy number, $Da = 10^{-4}$ - 10^{-1}) on the collector outlet temperature, i.e. overall heating of the working fluid (Prandtl number, $Pr = 7$), has been studied. Numerical experiments are performed by modifying a generic code (SimpleFOAM) from the OpenFOAM® repository with the extended Darcy-Brinkman-Forchheimer model for realising porous medium. Results indicate that significant augmentation in heat transfer can be achieved by increasing the number of blocks due to improved thermal mixing. The increment was prominent for higher values of the height of porous blocks. However, the pressure drop penalty has to be spent in such cases. The performance of the FPSC channel improves when the number of porous blocks is minimal, along with lesser height. The value is higher even than the case of a channel filled with a continuous porous layer of varying thickness. Overall, a better performance evaluation criteria value is reported for the insertion of the porous block in comparison to both, empty and filled porous FPSC channel. Detailed insights are further provided on the inclusion of the Forchheimer term while modelling the porous medium. For lower values of permeability, wherein the porous resistances are higher in amplitude, the results vary significantly for Darcy-Brinkman model in comparison to Extended Darcy-Brinkman-Forchheimer model. The manuscript provides an impetus for further experimental work on the present case, and assists to explore the performance improvement in an FPSC channel by insertion of the porous medium.

1. Introduction

Climate change has put us on our guards, while health-risks and environmental issues related to fossil fuel burning become more critical every day. Heatwave, the breakdown of ocean conveyor belt circulation and collapse of major ice sheets due to global warming are some of the vital concerns [1]. Scientists have been proposing suitable alternatives for decades now, and there has been extensive research on the proper methods of extraction of energy from non-conventional natural sources, like solar and wind energy. The population is ever-growing, and it is indeed essential to either switch entirely to or at least utilise partly, the various other methods of energy generation, keeping in mind the production of heat islands in major cities.

Out of the ever-lasting source of energies in nature, solar energy is considered to be the cleanest, which can be readily converted in a useful form. The reason is that solar thermal systems have been one of the most exciting technologies that interest engineers. One of the oldest solar thermal systems, the flat-plate solar collectors (FPSC), which is also the most applied one, exhibit a high amount of heat loss and minor thermal efficiency. Efforts have been laid on the various methods of improving and optimising thermal performance of the flat-plate collectors by using various methods, like inserting porous materials. Over the past few decades, FPSCs have been fine-tuned in several ways to enhance their overall performance. It is well-known that porous materials can be effectively

* Corresponding author.
E-mail addresses: ssdhinakar@gmail.com, sdhina@iiti.ac.in (S. Dhinakaran).

https://doi.org/10.1016/j.renene.2019.06.015
0960-1481/

Nomenclature

$\dot{Q}$	volume flow rate (lit/min)
d	diameter of the spherical particle of packed bed (m)
D_h	hydraulic diameter (m)
Da	Darcy number, κ/D_h^2
F	inertial factor, $(1.75/\sqrt{150})\cdot(1/\varepsilon^{1.5})$
f_D	dimensionless pressure drop (friction factor)
H	collector channel height (m)
k	thermal conductivity of the material $W/(m\cdot K)$
k_{eff}	effective thermal conductivity, k_e/k_f
L	collector channel length (m)
NP	Arragement of porous blocks, block absent at the inlet and present at the outlet
Nu	local Nusselt number, $-k_{eff}(\partial\theta)/(\partial Y)$
P	dimensionless pressure, $p/(U_\infty^2)$
p	kinematic pressure of the fluid, (m^2/s^2)
PN	Arragement of porous blocks, block present at the inlet and absent at the outlet
PP	Arragement of porous blocks, block present at the inlet and outlet
Pr	Prandtl number, ν/α
q_w	radiative heat flux (W/m^2)
Re	Reynolds number, $U_\infty\cdot D_h/\nu$
S	porous block height (m)
T	dimensional temperature, K
t	dimensional time, (s)
U, V	non - dimensional x, y - component of velocity, u/U_∞, v/V_∞
u, v	x, y - component of velocity (m/s)
X, Y	non-dimensional horizontal, vertical distance, x/L, y/H
x, y	horizontal, vertical distance (m)
c	order of accuracy of the schemes used, $(ln(f_3-f_2)/(f_2-f_1))/(ln(r))$
f	parameter value at respective grid size
F_s	factor of safety for predicting exact value by Richardson Extrapolation
f_{RE}	exact value predicted by Richardson Extrapolation, $f_1+(f_1-f_2)(r^c-1)$
GCI	Grid Convergence Index, $F_S\cdot(\phi)/(r^c-1)$
r	refinement ratio based on grid element size
Greek	
α	thermal diffusivity (m^2/s)
ε	porosity
κ	permeability of the material (m^2)
ν	kinematic viscosity (m^2/s)
ρ	density (kg/m^3)
τ	non-dimensional time, $t\cdot U_\infty/D_h$
θ	non-dimensional temperature $(T-T_\infty)/(T_w-T_\infty)$
ϕ	relative error between parameter values at a specific grid size
Subscript	
∞	far field value
eff	effective value
in	inlet value
1, 2, and 3	fine, medium, and coarse grid values

used as a passive way of improving heat transfer, and they have always attracted researchers in the past few decades. In particular, porous metal foams, are of prime importance in solar thermo-chemical reactors and thermal collectors. Due to the presence of voids, porous materials have been used to store thermal energy and enhance thermal mixing (promotes thermal conductivity of the fluid) and, to control flow instabilities like vortex shedding [2]. For instance, on placing a porous layer near the wall of a channel, a higher thermal gradient can be achieved at the wall, resulting in lower thermal resistance to the flow. Also, if the heat is first conducted through a material, across which the circulating fluid can pass, heat absorption should considerably increase. Hence, it would be further interesting to look for possibilities of design uplifting in solar collectors or heat exchangers by inserting porous metal foam in the channel.

Huang and Vafai [3] numerically explored forced convection augmentation in a channel using multiple emplaced porous blocks. The vortices were controlled by altering governing parametric values, and this had significant effects on heat transfer characteristics. However, a significant increment in pressure drop due to porous blocks is also reported. Chikh et al. [4] carried out a numerical study for flow across porous blocks with a heat source at their bottom in a channel. Darcy number was varied from 10^{-5} to 10^{-2} and Reynolds number was increased up to $Re = 1500$. The number of blocks was varied up to 9, and the effect of their height was also studied. In the presence of porous blocks, the shear stress reduces at the lower wall. Also, heat transfer was found to enhance by usage of blocks in an intermittently heated channel. A steep downfall in the wall temperature may be obtained of about 90%. Guerroudj and Kahalerras [5] studied mixed convection in a channel with heated porous blocks of various shapes with a local heat source. The numerical analysis was carried out at various values of Richardson number $(Ri) = 0–20$, Darcy number $(Da) = 10^{-6}$ - 10^{-1}, Reynolds number $(Re) = 10–300$, and thermal conductivity ratio $R_k = 1–10$. Presence of porous blocks was seen to affect the flow structure immensely, which in turn affects the heat transfer rate. For increasing Ri, lower permeability, Reynolds number, porous block height, and thermal conductivity ratio values, and triangular shape of the porous bluff obstacle, Nusselt number increases significantly. Authors claim that inserting intermittent porous blocks results in an increment in friction factor value. Buoyancy, however, was not seen to affect the friction coefficient much. Further, Authors [6] studied mixed convection in an inclined channel provided with porous heated blocks on its lower plate. The comparison of the net energy gain (or energy loss) to the generated pressure drop showed that high heat transfer and low-pressure drop are secured for positive inclination angles with reduction of this range of angles when the permeability of the porous blocks is reduced. Chen and Huang [7] carried out a numerical analysis for higher heat transfer from a strip heat source, kept in a solar channel, by discrete metal-foam blocks. Insertion of metal-foam blocks at the inner wall of absorber turned out to be an effective method of improving the thermal performance of the channel. With proper optimisation of the porous block properties, and adjusting the pressure drop accordingly, thermal efficiency also can be increased due to the presence of metal-foam block. Huang et al. [8] inserted four metal blocks at the inner side of the absorber wall and subjected them to pulsating flow. In their numerical analysis, this method of enhancing heat transfer between the absorber and working fluid was declared to be efficient. Chen et al. [9] presented a numerical study of forced convection in a partial-full metal-foam porous channel with discrete heat sources on the bottom wall. Authors claim that local thermal equilibrium assumption holds for higher heat exchange between the fluid and porous surfaces, and lower porosity values. Mean Nusselt number was reported to be higher at lower porosity than higher porosity. An increment of 17% is obtained at 40PPI, in comparison to 5PPI. It was stated that enhancement in heat transfer is always accompanied by an increase in pressure drop as a penalty. The pressure drop was told be higher at higher pore density, lower permeable, smaller porosity, or fibre diameter of metal foams. In another study [7], it is shown that there exists a critical value of Da at which minimum heat transfer enhancement is shown. It should be noted that in all the above studies, the porous blocks are placed close to each other in a limited space in the channel.

Extensive literature is available on porous substrates being introduced in the collector channel for improvement in thermal performance. Lansing et al. [10] analytically and experimentally studied the performance of a porous FPSC by inserting a porous substrate diagonally across the channel. Their analysis showed that considerable improvement in performance could be obtained by using porous insertion and the increment can be as much as 102%. Chen et al. [11] performed analysis of energy storage process an FPSC with an integrated aluminium foam filled with paraffin as the

phase-change medium. Two-temperature model is used to realise heat transfer between metal foams and paraffin. Results suggest the usage of non-thermal equilibrium is more appropriate than the equilibrium assumption for modelling phase-change material in porous foam. Further, heat transfer performance was reported to significantly improved by using aluminium foam filled with paraffin. Rashidi et al. [12] provide sensitivity analysis on the influence of Darcy number, Reynolds number, porous substrate thickness on the combined convection-radiation heat transfer in a heat exchanger filled with a porous medium of different thickness. The sensitivity analysis reveals that Reynolds number affects pressure drop and Nusselt number lesser at high Darcy number and porous medium thickness values. Also, the Nusselt number is sensitive to the porous substrate thickness at higher thickness values. Bovand et al. [13] analyse combined convection-radiation heat transfer in a porous FPSC with varying porous layer thickness. It is seen that the Nusselt number increases with the porous layer thickness at higher values of Darcy number, while at lower Darcy number the converse is true. The average Nusselt number is reported to increase with the radiation parameter. Jouybari et al. [14] carried out an experimental investigation on the thermal performance and the pressure loss of an FPSC with a fully filled porous channel. The results suggest that the insertion of porous foam increases optical efficiency and reduces heat losses in the lower values of the Reynolds number. The reason for this occurrence is told to be the improvement in solar energy absorption potential of the working fluid. An increment of 82% in Nusselt number is obtained by inserting the porous substrate. However, higher pumping power is demanded to achieve this rise, due to the increase in pressure drop across the channel. Still, the surge is not declared to be significant to go for a greater electrical pump. Furthermore, Authors [15] carried out an experimental study on the thermal performance of a fully filled porous FPSC with SiO_2/deionised water nanofluids. They have reported that the porous channel with nanofluids provided higher heat transfer but also resulted in a significant pressure drop. Overall, the performance of the porous channel with nanofluids was found to be lower than the empty channel with nanofluids. In another analytical study [16] of the heat transfer in a thin FPSC with a fully saturated porous channel considering the influence of solar radiation. They reported that both porous shape parameters and radiation have a significant impact on collector thermal performance, while the influence of radiation being more pronounced. Pressure drop was found to be negligible at smaller values of porous insertion properties. Saedodin et al. [17] analysed the performance of an FPSC filled with porous metal foam. Their results suggest that higher thermal performance is obtained when the channel is fully filled with a porous substrate. However, with respect to the empty channel, the performance of the porous channel was reported to be lower. Insertion of porous foam was resulting in a significant enhancement in Nusselt number up to 82%, but pressure drop also increased significantly. Ameri and Eshaghi [18] introduced a novel system utilising Fe_3O_4/Water nanofluid in porous media at a constant magnetic field in the FPSC absorber tube. An increment in Nusselt number by 1.36 times was reported with respect to the conventional collector. Also, an enhancement in performance was recorded, with the Performance Evaluation Criteria (PEC) values of 1.319. It is important to understand that the experimental studies detailed above for solar collectors, considered only limited lower values of porous foam permeability.

From the above review, it is clear that the insertion of a porous medium in FPSC channel results in an increment of heat exchange between the incident solar radiation and the working fluid. The pressure-drop penalty to be paid does not appear to be dominant to demand higher pumping. It is also apparent that the insertion of intermittent porous blocks in the collector channel promotes improved thermal mixing, due to the recirculation occurring between the porous blocks. It is well-known that the performance of a flat-plate solar collector can be improved by using obstacles like discs, wire coils, twisted tapes, metal foams, etc. The thermal boundary layer thickness reduces, and turbulence and swirling flow increases because of such insertions. Furthermore, if this obstacle is porous material with higher thermal conductivity and permeability, the flow mixing increases and the pressure drop decreases [19]. However, to the best of Authors' knowledge, there exists no study which comments on the performance improvement of an FPSC channel due to insertion of porous blocks spanning throughout the channel length. Also, the influence of the presence or absence of porous blocks at the inlet and/or outlet of the channel is unexplored. The optimum number of porous blocks for attaining maximum thermal mixing, better performance, and lesser pressure drop loss has not been studied. The impact of the flow dynamics around porous blocks spanning throughout the channel, at different values of permeability, height, number, and presence/absence at the channel inlet/outlet is investigated in the present numerical endeavour. The primary aim of the study is to predict the configuration at which maximum thermal performance can be achieved by tweaking with the parameters as mentioned earlier. Also, a comment on the inclusion of the Forchheimer term in the modelling of porous metal foam is given, which has not been provided in the literature. The numerical results presented in this manuscript shall give an impetus for experimental efforts in the insertion of the porous blocks of various porous properties and configurations.

2. Mathematical formulation

2.1. Problem description

Numerical simulations have been carried out for laminar, incompressible and steady flow through a two-dimensional FPSC channel, which is filled with metal-foam blocks as shown in Fig. 1. The fluid is assumed to be water with a Prandtl number, *Pr* value of 7. Dimensions of FPSC are inspired by the combined numerical and experimental study by Saedodin et al. [17]. Channel length and height are set to 0.8 m and 0.013 m, respectively. The thickness and optical properties of glass and absorber plate are neglected, and they both are assumed to be a single layer similar to several numerical works on FPSC channels [12,13,17]. Porous metal foam blocks with uniform porosity and permeability are inserted intermittently into the FPSC with various permutations and combinations. The fluid (water) enters the domain with a uniform velocity distribution (U_∞) and a constant temperature (T_∞). A constant flow rate of 0.5 lit/min, corresponding to a Reynolds number value of around 117, is considered. At the upper absorber plate, a uniform heat flux (q_w) is incident along the entire channel length, which represents the solar insolation. In order to make the current problem amenable for numerical simulations, it is assumed that the porous insertion is homogeneous and isotropic and is saturated with a single-phase fluid. Fully developed flow is desired in the porous channel, while fluid and solid temperature are expected to be equal, i.e. local thermal equilibrium (LTE) condition is assumed. This condition can be safely taken in cases where slow warming exists, like the present case of warming of water. Absorber plate, glass plate, and an intermediate layer is assumed to be a single plate of uniform thermal properties. The dimension of this particular layer is small in comparison to the entire channel height and is, therefore, overlooked during simulations. Solar insolation incident on absorber plate of the channel is uniformly distributed over the full length and is constant in amplitude for the entire run.

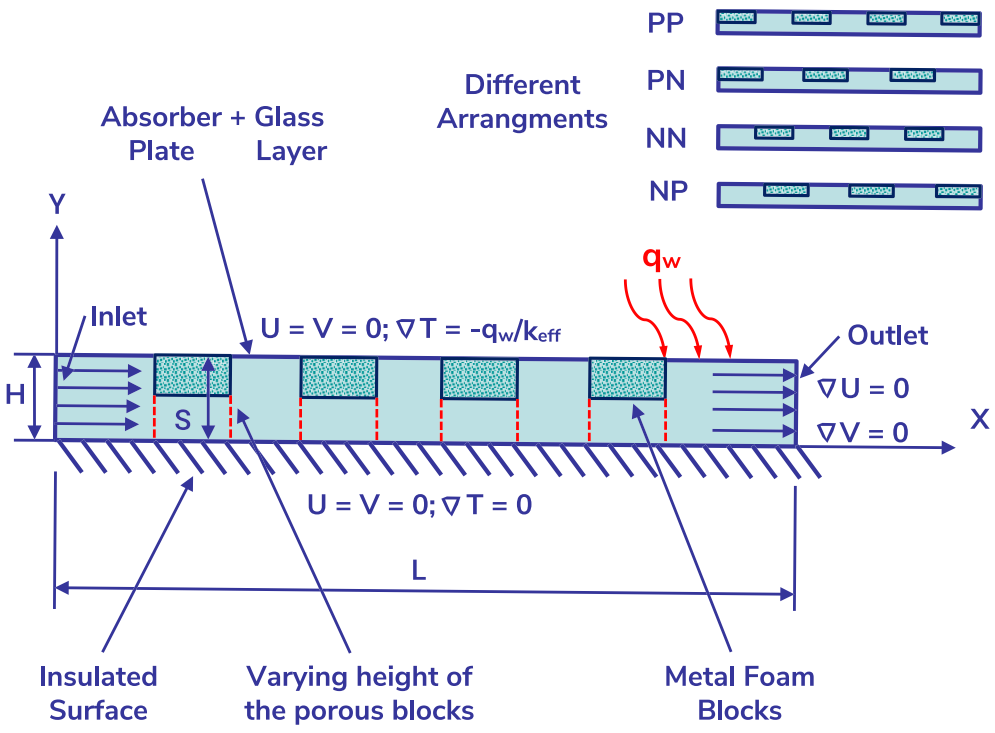

Fig. 1. Schematic of the computational setup for the flow through FPSC, along with boundary condition details, exposed to solar radiation and inserted with intermittent porous blocks.

2.2. Governing equations

Considering the assumptions as mentioned earlier, flow and heat transfer in the porous medium inside the channel can be modelled by.

Continuity Equation:

$$\frac{\partial u}{\partial x}+\frac{\partial v}{\partial y}=0, \tag{1}$$

Momentum Equations:

$$\frac{\rho}{\varepsilon^2}\left(u\frac{\partial u}{\partial x}+v\frac{\partial u}{\partial y}\right)=-\frac{\partial p}{\partial x}+\frac{\mu_e}{\varepsilon}\left(\frac{\partial^2 u}{\partial x^2}+\frac{\partial^2 u}{\partial y^2}\right)-\frac{\mu}{\kappa}u-\frac{\rho F}{\sqrt{\kappa}}|\vec{V}|u, \tag{2}$$

$$\frac{\rho}{\varepsilon^2}\left(u\frac{\partial v}{\partial x}+v\frac{\partial v}{\partial y}\right)=-\frac{\partial p}{\partial y}+\frac{\mu_e}{\varepsilon}\left(\frac{\partial^2 v}{\partial x^2}+\frac{\partial^2 v}{\partial y^2}\right)-\frac{\mu}{\kappa}v-\frac{\rho F}{\sqrt{\kappa}}|\vec{V}|v, \quad \text{and,} \tag{3}$$

Energy Equation:

$$\frac{1}{\varepsilon}\left(u\frac{\partial T}{\partial x}+v\frac{\partial T}{\partial y}\right)=\alpha\left(\frac{\partial^2 T}{\partial x^2}+\frac{\partial^2 T}{\partial y^2}\right) \tag{4}$$

In the above equations, $\left|\vec{V}\right|=\sqrt{u^2+v^2}$ is the resultant velocity and $F=\frac{1.75}{\sqrt{150}}\cdot\frac{1}{\varepsilon^{1.5}}$ is the inertial factor [20-23].

2.3. Non-dimensionalisation of results

Using non-dimensional variables in OpenFOAM 5.0 is quite cumbersome, and hence, non-dimensionalisation of the output variables is done post-simulation, by using the following characteristic scales

$$X=\frac{x}{L}, Y=\frac{y}{H}, P=\frac{p}{\rho U_\infty^2}, U=\frac{u}{U_\infty}, V=\frac{v}{U_\infty} \quad \text{and} \quad \theta=\frac{T-T_\infty}{T_w-T_m}. \tag{5}$$

2.4. Boundary conditions

The boundary conditions applied to the computational domain are displayed in Fig. 1. Uniform flow is incident at the inlet of the porous FPSC, at an ambient temperature, written as $U=U_{in}$, $V=0$, $T=T_{in}$ and $\nabla P=0$. The 'inletOutlet' boundary condition is used at the outlet of the domain. This treatment gives a fully developed condition in terms of $(\partial U)/(\partial X)=0$, $V=0$, $\nabla T=0$ and $P=0$. In the case of any reversal in the flow direction, the velocity is automatically set to a fixed value (which is 'zero', as in real condition no backflow is expected to occur). The bottom of porous FPSC channel is insulated to avoid heat losses and a 'no-slip' boundary condition is imposed by $U=V=0$, $\nabla P=0$ and $\nabla T=0$. The top wall is exposed to solar radiation heat flux 'q_w' [24,25], while 'no-slip' boundary condition is imposed throughout the wall by $U=V=0$, $\nabla P=0$ and $\nabla T=-q_w/k_{eff}$.

3. Numerical details

For modelling flow and heat transport in a metal-foam filled porous FPSC, numerical simulations are performed using the finite volume method, and the open source tool OpenFOAM® [26] is used. The generic 'SimpleFoam' solver (by inserting temperature field additionally) of OpenFOAM® is improvised by applying the Darcy-Forchheimer-Brinkman model. This solver is robust in handling laminar and steady problems and hence, is chosen for the present computations. The steady-state scheme is used to account for the time derivative, while Gauss linear scheme is used for the gradient, divergence (bounded type) and Laplacian terms and a linear

interpolation scheme is used for the collocated grid. Further, PCG solver with DIC pre-conditioner is used for the pressure term, and PBiCG solver with DILU pre-conditioner is used for evaluating the velocity and temperature terms. Although OpenFOAM® does not use an explicit Rhie-Chow correction, the generic correction for pressure terms is believed to be 'Rhie-Chow inspired' [27]. The residual criteria for pressure, velocity and temperature terms is set to 10^{-6}. An under-relaxation of 0.3, 0.7 and 0.98 are applied for pressure, velocity and temperature terms, respectively.

4. Grid generation and code validation

The generic blockMesh tool of OpenFOAM 5.0 is used for the generation of structured uniform mesh in the computational domain. In order to verify the independence of the grid in usage, the grid dependence test is carried out at extremities of the variable values considered in the study. The test is carried out for Case 4, $S = 0.2H$, NN arrangement, and $Da = 10^{-4}$. The analysis is carried out lower values of permeability keeping in mind that at such values, the viscous and inertial resistance to flow is higher in comparison to permeability values above $Da \geq 10^{-4}$. Also, the grid has to be sufficiently fine to capture the flow physics of thin porous blocks placed near each other, and hence, $S = 0.2$H and Case 4 are considered. The variations in local Nusselt number (Nu), friction factor (f_D), and maximum temperature (θ_{max}) and maximum horizontal velocity (U_{max}) at the outlet are checked. The quantitative grid verification has been performed using the grid convergence index (GCI). For deciding on the choice of the grid to be used in the

Table 1
Grid dependence study details provided for $Da = 10^{-4}$, $S = 0.2H$, NN configuration, and Case 4. Grid Convergence Index (GCI) is provided along with f_{RE} calculated by Richardson Extrapolation Method [1]. E_{RE} is calculated with respect to f_{RE}, while GCI is calculated for relative error between grid values for local Nusselt number (Nu), friction factor (f_D), and maximum temperature (θ_{max}) and maximum horizontal velocity (U_{max}) at the outlet of flat-plate solar collector channel.* represents chosen Grid for the study.

Grid (M x N)	E_{RE} (%)	Nu	GCI (%)	E_{RE} (%)	f_D	GCI (%)	E_{RE} (%)	θ_{max}	GCI (%)	E_{RE} (%)	U_{max}	GCI (%)
A (75×50)	4.9296	14.0592	1.7254	4.1420	0.3078	1.4351	0.5939	1.2365	0.1885	0.0853	1.5236	0.0314
B (150×100)	2.3465	13.7131	1.0498	2.0866	0.3144	0.7739	0.3173	1.2331	0.1222	0.0393	1.5243	0.0179
C (300×200)*	0.7986	13.5057	0.3521	0.9654	0.3180	0.4273	0.1383	1.2309	0.0611	0.0131	1.5247	0.0045
D (600×400)	0.2821	13.4365	–	0.3426	0.3200	–	0.0488	1.2298	–	0.0066	1.5248	–
f_{RE}	–	13.3987	–	–	0.3211	–	–	1.2292	–	–	1.5249	–

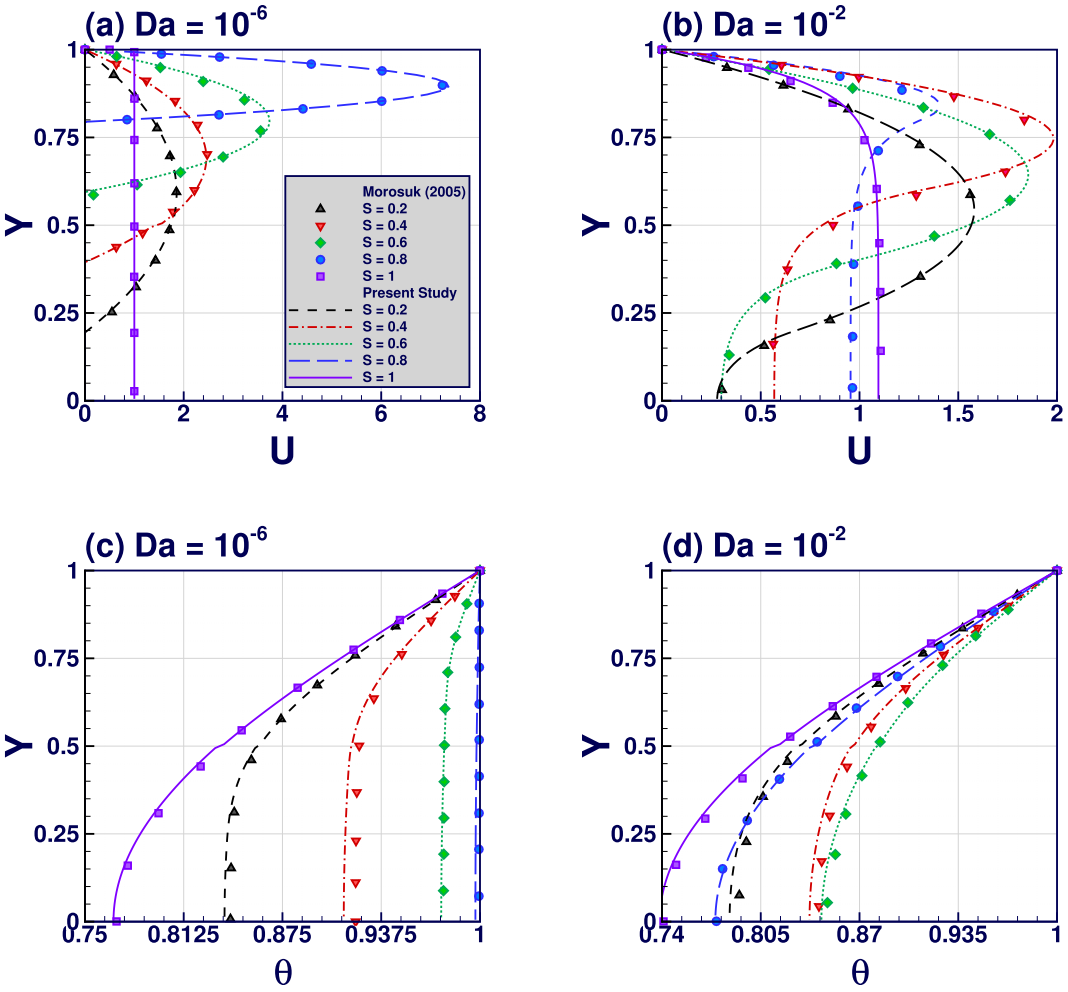

Fig. 2. Comparison of horizontal velocity and temperature profiles at the outlet of the porous channel with [29] at various Darcy number (Da) and porous block height (S) values.

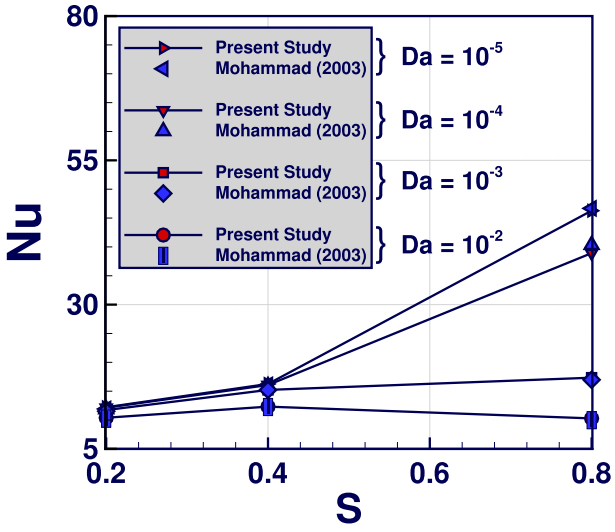

Fig. 3. Comparison of local Nusselt number (Nu) calculated at the top right corner of the porous channel with [27] at various Darcy number (Da) and porous block height (S) values.

study, the Grid Convergence Index (GCI) provided by Roache [28] is used, which is based on generalised Richardson Extrapolation involving the comparison of discrete solutions at two different grid spacings. An exact solution based on the Richardson Extrapolation is also estimated, and relative error with respect to this value is given. Usually, three values of variables at three different grid refinements are considered as f_1, f_2, and f_3 for fine, medium, and coarse grid structures, respectively. GCI for medium grid with respect to fine grid is defined as,

$$GCI^{12}(\%) = 100 \cdot F_S \cdot \left(\frac{\phi}{r^c - 1}\right) \tag{6}$$

where F_S = factor of safety (usually kept to be 1.25), r = refinement ratio (in the present case it is '2'), $\phi = (f_2 - f_1)/f_1$ and c = order of convergence (in the present case it is taken to be '1.5'). The order of convergence, c, is then written as,

$$c = \frac{ln\left(\frac{f_3 - f_2}{f_2 - f_1}\right)}{ln(r)} \tag{7}$$

Similar logic follows for GCI for coarse grid with respect to medium grid (GCI^{23}). Current solver is tested for four different grids of X × Y sizes viz., 75 × 50 (Grid A), 150 × 100 (Grid B), 300 × 200 (Grid C) and 600 × 400 (Grid D). Details of the grid dependence study is given in Table 1. Relative error (E_{RE}) is also given for various variables at different Grid resolutions with respect to the exact value predicted by Richardson Extrapolation by using,

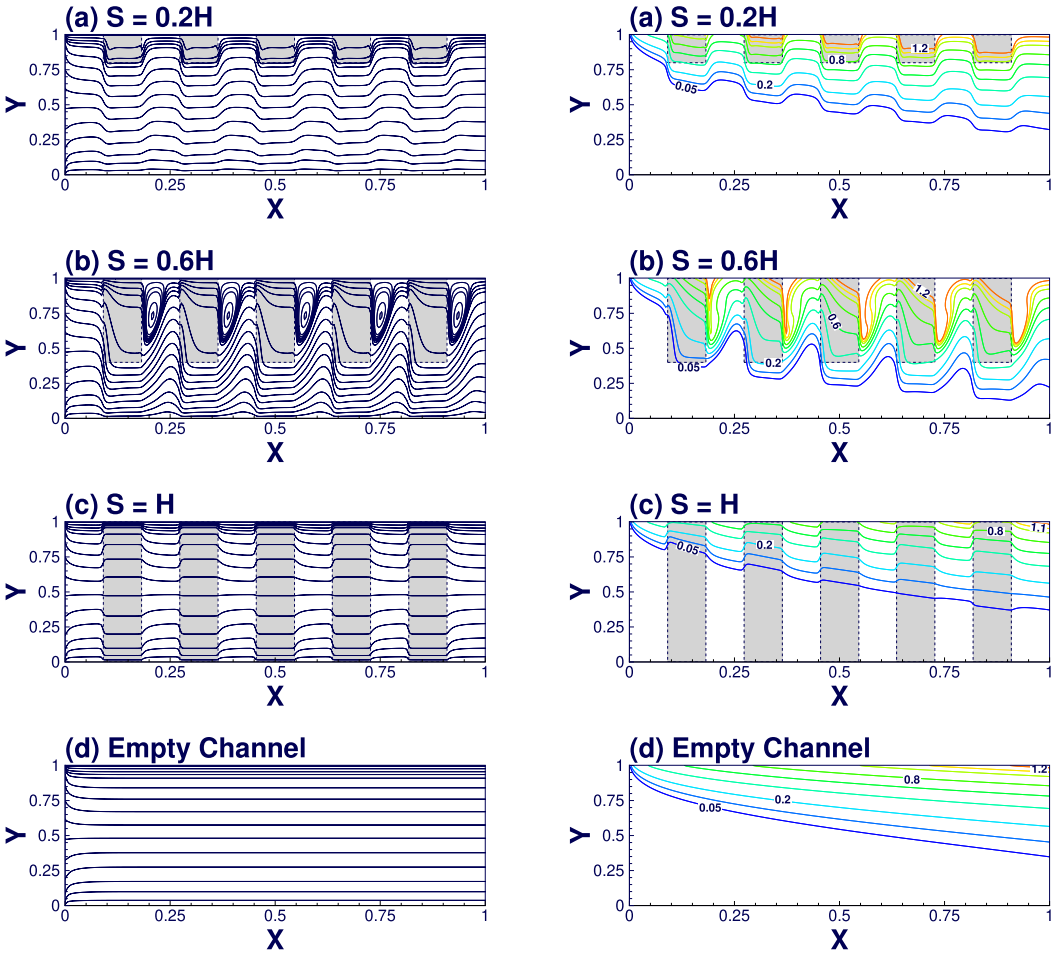

Fig. 4. (I) Streamline and (II) Isotherm contours around porous blocks for various values of porous block height (S), shown at Darcy number, $Da = 10^{-3}$, Case 3 and NN configuration.

$$f_{RE} = f_1 + \frac{f_1 - f_2}{r^c - 1} \tag{8}$$

The current solver is verified with the numerical results of Morosuk [29] at the various thickness of the porous layer and *Da*, and satisfactory confidence is obtained. Both temperature and velocity profiles showed good agreement with their experimental results, which is detailed in Fig. 2. Furthermore, the present numerical recipe is tested for Nusselt number variation with the numerical work by Mohamad [30] (see Fig. 3). The local *Nu* at the right corner of the top wall of the porous channel shows acceptable closeness. Sufficient confidence is achieved in the present numerical code by this two-fold validation, allowing to proceed ahead with the numerical experiments.

5. Results and discussions

Extensive two-dimensional numerical computations are carried out for understanding the influence of porous blocks' number, arrangement, thickness, and *Da*, on the flow patterns and heat transfer performance of a solar flat plate collector filled with porous metal foam blocks. The following range of parameters is considered during simulations:

- Darcy number, $Da = 10^{-4}$, 10^{-3}, 10^{-2}, and 10^{-1}.
- Porous blocks' height, $S = 0$, $0.2H$, $0.4H$, $0.6H$, $0.8H$, and H.
- Arrangement of porous blocks, NN (porous block absent at the inlet and the outlet), NP (porous block absent at the inlet and present the outlet), PN (porous block present at the inlet and absent the outlet), and PP (porous block present at the inlet and the outlet).
- Number of porous blocks, Case 1 (one block), Case 2, (three blocks), Case 3 (five blocks), and Case 4 (seven blocks). (Note: For PP arrangement, one more block shall be included)

5.1. Streamline and isotherm contours

When the water flows into the FPSC channel filled with porous metal foam blocks, after travelling a certain distance, a fully developed condition is established before the flow reaches the outlet of the collector. The channel is kept long enough for the flow to attain a fully developed condition. It should be noted that four different cases depending on the number of porous blocks are considered in the present study viz., Case 1, Case 2, Case 3, and Case 4. These cases represent 1–2, 3–4, 5–6, and 7–8 porous blocks, respectively. Depending on the arrangement, the number of porous blocks may vary. For instance, Case 3 consists of five blocks for NN, NP, PN arrangements, while six blocks for PP arrangement. A similar relation exists for all the cases, wherein only for PP arrangement, an extra block exists. For the sake of convenience, the aspect ratio of the channel has been changed for proper representation of contours, but the reader should understand that the channels are long

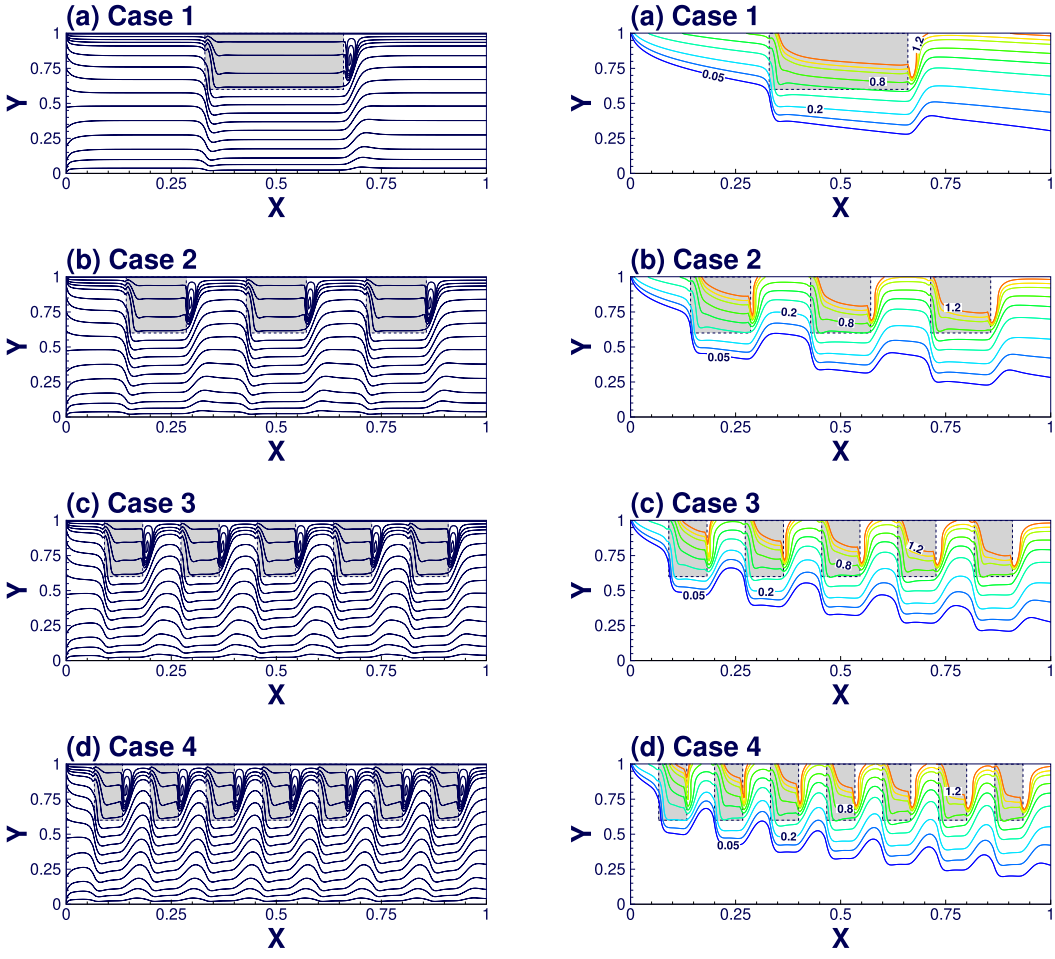

Fig. 5. (I) Streamline and (II) Isotherm contours around porous blocks for various cases, shown at porous layer thickness, $S = 0.4$, Darcy number, $Da = 10^{-3}$ and NN configuration.

and thin, and so are the blocks.

In Fig. 4, streamline and isotherm contours are shown for various values of S, and a comparison with empty channel is given in Fig. 4(d). The contours are plotted at $Da = 10^{-3}$ for Case 3 and NN configuration. When the height of porous blocks is smaller, very little or no recirculation exists, but the presence of blocks is apparent through deviated streamlines throughout the channel (Fig. 4(I)), when compared with the empty channel. As S increases, fluid flow is disrupted and a vortex forms behind each porous block, which restrict itself close to the rear end of the respective block, without impinging on the surface of the next block. The height of this recirculation region increases with S, until it completely vanishes for $S = 1$, wherein the flow remains uniformly distributed and undisturbed while it flows downstream towards the outlet. Effect of the flow on the thermal field can be seen in Fig. 4(II). The primary aim of placing porous material near the absorber wall is to enable the storage of thermal energy in the void-filled foam blocks, which later can be imparted to the working fluid so that maximum outlet temperature can be achieved. In comparison to the empty channel, intermediate S values offer higher outlet temperature, along with a thinner thermal boundary layer at the outlet. Fully occupied and lesser values of S provide smaller outlet temperature and a thicker thermal boundary layer at the outlet of the channel.

Effects of the number of porous blocks on flow and heat transfer are shown in Fig. 5(I) and (II), respectively. The contours are plotted at $S = 0.4$, and $Da = 10^{-3}$ for NN arrangement. It is clear that, as said before, even after increasing the number of blocks, recirculation region restricts near the rear face of each porous block. Such an occurrence may be due to the fixed flow rate and the tendency of the fluid flow to follow a path of least resistance and escape through the gap between the insulator plate and block. The increased mixing is reflected well in the thermal contours, wherein an increased temperature distribution in the clear for Case 4 in comparison to Case 1. Higher outlet temperature is observed for Case 4, and a thinner boundary layer exists.

Contours for various arrangements of porous blocks are shown in Fig. 6, for Case 3, $S = 0.4$, and $Da = 10^{-3}$. Again, regardless of arrangement, the recirculation region is localised to each block, assuring a steady and uniform flow throughout the channel. Thermal contours, however, show some interesting phenomenon. When the porous block is absent at the outlet of the channel, as seen through Fig. 6(II)(a) and (c), higher outlet temperature, along with thinner thermal boundary layer is evident. On the contrary, when a porous block occupies the outlet, a thick thermal boundary layer is witnessed, and a lesser value of outlet temperature is obtained. As a result, lower heat transfer rate and hence, a lesser thermal performance can be predicted at these configurations.

At various Da values, fluid flow and heat transfer are well-studied and present results agree with the natural behaviour, as displayed in Fig. 7. As permeability of the porous blocks increases, more amount of fluid flow occurs through the medium, which diminishes the recirculation region. Since, this condition demotes

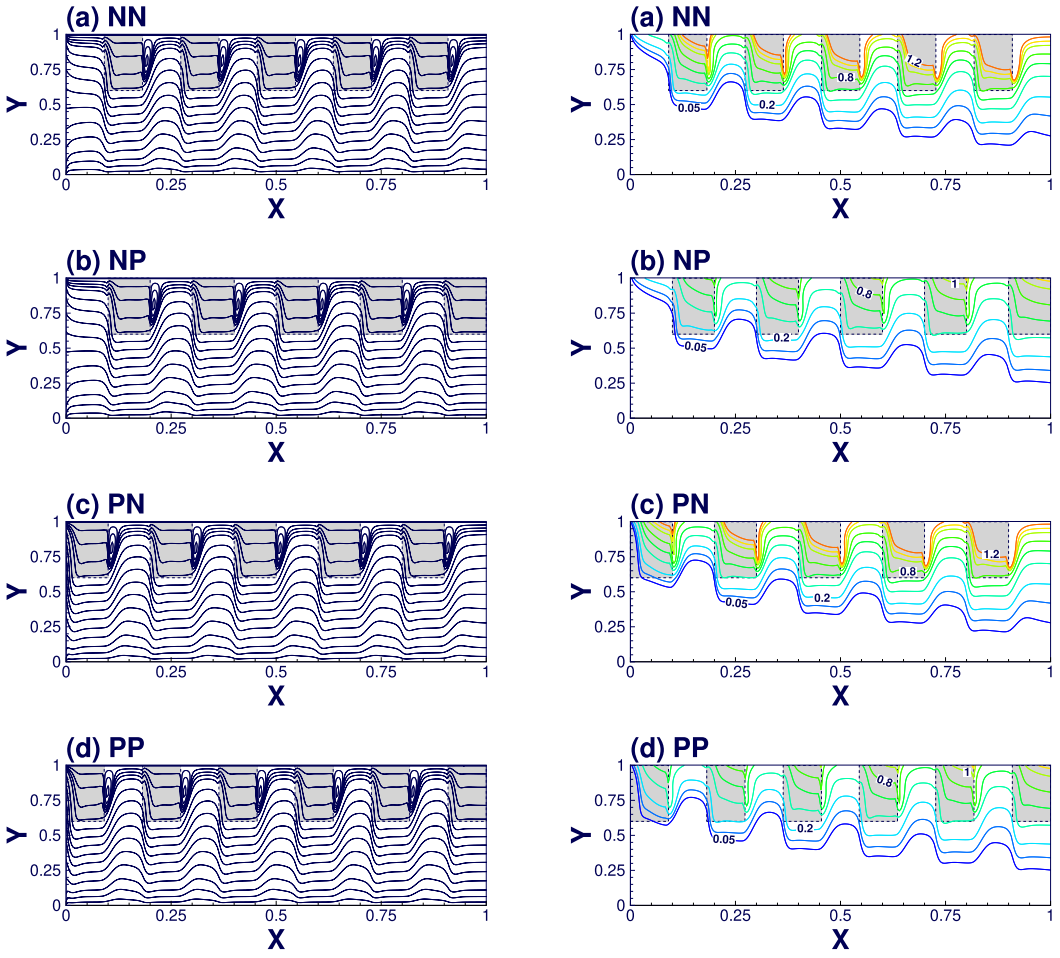

Fig. 6. (I) Streamline and (II) Isotherm contours around porous blocks for various arrangement of porous blocks, shown at porous layer thickness, $S = 0.4$, Darcy number, $Da = 10^{-3}$ and Case 3.

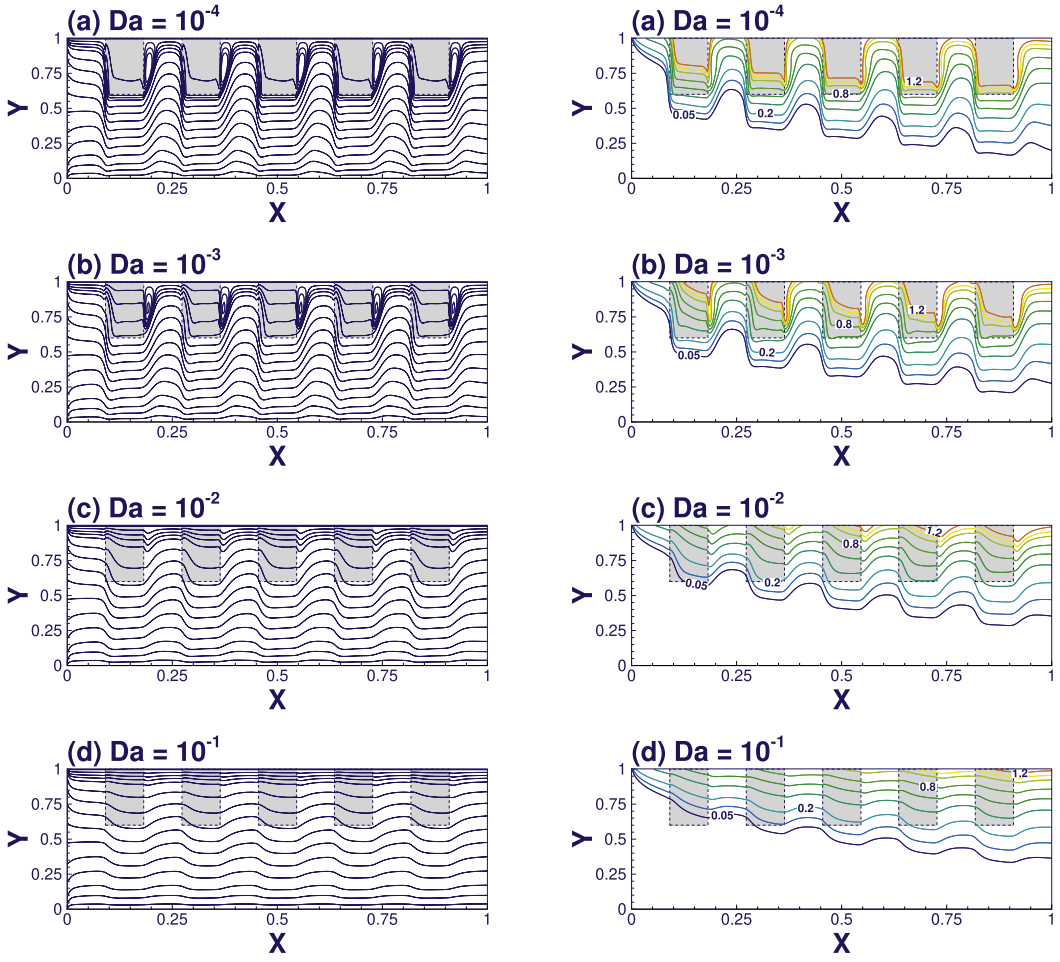

Fig. 7. (I) Streamline and (II) Isotherm contours around porous blocks for various Darcy number (*Da*), shown at porous layer thickness, $S = 0.4$, NN configuration, and Case 3.

thermal mixing and takes the channel to an empty-like situation, lesser outlet temperature and more uniform thermal contours are noticed. A decrement in heat transfer rate must occur due to these occurrences, and the details are given below.

5.2. Local Nusselt number variation

Post-solving the governing equations numerically, heat transfer at the top-right corner of the outlet of FPSC is quantified through the local Nusselt number. The local *Nu* is evaluated by the weighting of temperature with velocity field as demonstrated in the literature as [17],

$$Nu = \frac{D_h}{T_w - T_m(x)} \left(\frac{\partial T}{\partial y}\right)_{y=H}. \tag{9}$$

In the above equation, $T_m(x)$ is the fluid bulk temperature and it is obtained as follows:

$$T_m(x) = \frac{\int_{y=0}^{y=H} uTdy}{\int_{y=0}^{y=H} udy} \tag{10}$$

An overall influence of flow dynamics as mentioned earlier is witnessed on the variation of local Nusselt number through Fig. 8 and Table 2. The trends of *Nu* are shown for Cases 1 and 4, $S = 0.2H$ and H, and various arrangements considered. Overall, as predicted earlier, when the porous block is absent at the outlet, a higher heat transfer rate at the outlet is achieved. The only exception being $S = H$, wherein PP and NP arrangements show higher *Nu* values. As at this condition, there exists no mixing due to absent recirculation, the higher surface area available at the inlet and outlet for fluid to exchange heat with porous media aids the heat transfer. However, one should suspect a higher need for pumping power due to greater resistance to offer. With *Da*, *Nu* increases for PP and NP arrangements, while it decreases for NN and PN arrangements. When *Da* increases, flow tends to flow through porous media, resulting in lesser thermal mixing. As a result, for NN and PN arrangements, *Nu* decreases.

When comparing several cases considered in the study, including completely filled, empty, and the channel filled with the porous layer, NN arrangement provided maximum *Nu*, which is given in Table 2. A peculiar trait in *Nu* is found for $S = 0.8H$, where high values are marked for $Da = 10^{-4}$, and sudden downfall occurs for $Da = 10^{-3}$, followed by a linear trend like elsewhere. The drop in values for $Da = 10^{-3}$ gets steeper as the number of blocks increase. Authors suspect that this trend must be related to the 'jump' occurring at intermediate permeability levels, reported earlier in literature for blunt porous bluff bodies [31,32]. Nevertheless, the long-standing recirculation region at $S = 0.8H$ and $Da = 10^{-4}$ enhances thermal mixing, which intensifies even further with the number of porous blocks. Local *Nu* values of 36.683 and 26.608 are reported for Cases 4 and 3, respectively for this particular setup. The

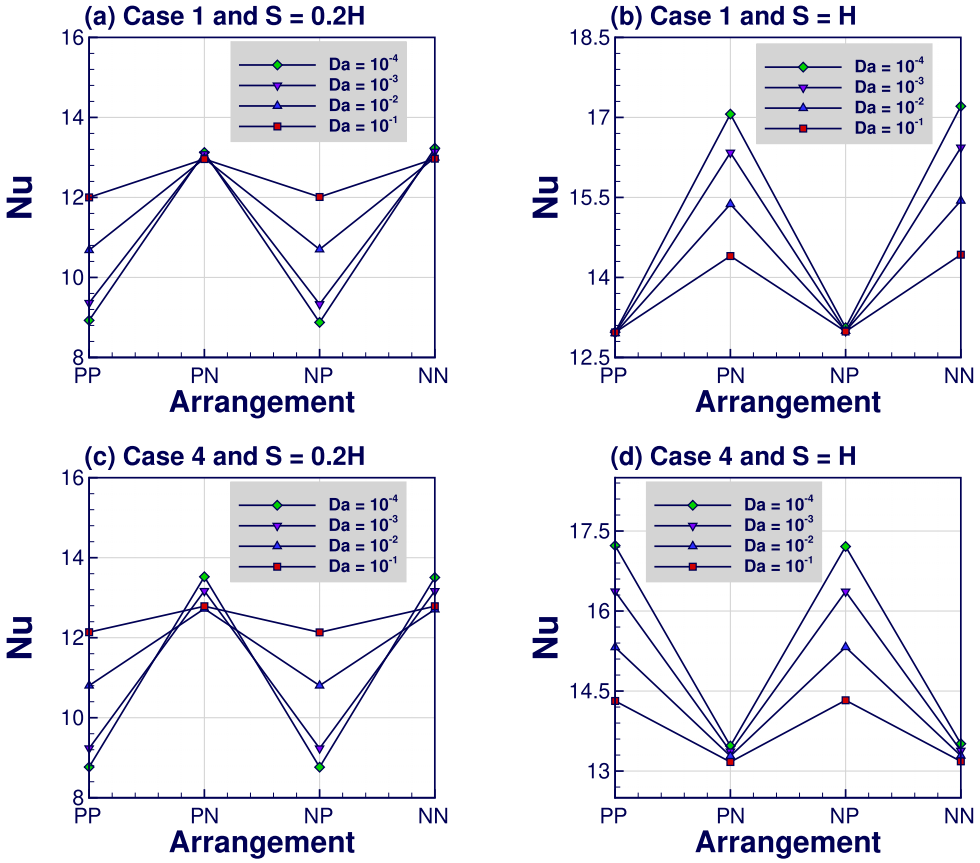

Fig. 8. Variation of local Nusselt number (Nu) calculated at the top right corner of the FPSC channel filled with blocks at various parameters.

Table 2
Local Nusselt number (Nu) calculated at the top right end of the FPSC channel and friction factor (f_D) for NN configuration at various values of porous block height (S), Darcy number Da and the number of porous blocks.

		Nu					f_D				
	Da	$S = 0.2H$	$S = 0.4H$	$S = 0.6H$	$S = 0.8H$	$S = H$	$S = 0.2H$	$S = 0.4H$	$S = 0.6H$	$S = 0.8H$	$S = H$
Case 1	10^{-4}	13.230	13.619	14.146	13.980	12.973	0.279	0.464	1.207	7.218	68.351
	10^{-3}	13.144	13.284	13.007	12.273	12.960	0.268	0.430	1.007	3.813	9.466
	10^{-2}	12.996	12.769	12.426	12.711	12.955	0.246	0.357	0.661	1.426	1.958
	10^{-1}	12.968	12.754	12.681	12.887	12.970	0.229	0.290	0.423	0.609	0.672
Case 2	10^{-4}	13.426	14.237	15.585	16.848	13.099	0.300	0.564	1.634	9.963	87.185
	10^{-3}	13.237	13.404	13.062	11.129	13.052	0.286	0.518	1.352	5.033	12.054
	10^{-2}	12.913	12.330	11.612	12.497	13.039	0.256	0.412	0.833	1.793	2.451
	10^{-1}	12.892	12.434	12.340	12.868	13.028	0.233	0.316	0.494	0.725	0.802
Case 3	10^{-4}	13.505	14.505	17.041	26.608	13.303	0.312	0.621	1.896	11.592	93.728
	10^{-3}	13.223	13.270	12.939	9.916	13.228	0.295	0.569	1.564	5.625	12.976
	10^{-2}	12.797	11.817	10.926	12.404	13.176	0.261	0.442	0.925	1.944	2.630
	10^{-1}	12.838	12.139	12.124	12.906	13.112	0.235	0.329	0.527	0.770	0.850
Case 4	10^{-4}	13.506	14.665	20.182	36.383	13.512	0.318	0.658	2.060	12.525	94.814
	10^{-3}	13.167	13.087	13.296	9.025	13.382	0.299	0.603	1.699	5.916	13.157
	10^{-2}	12.706	11.374	10.460	12.385	13.288	0.263	0.460	0.974	1.996	2.669
	10^{-1}	12.787	11.955	12.025	12.956	13.182	0.235	0.336	0.541	0.783	0.862

enhancement is prominent when compared with Nu values of 6.497 and 17.756 for the empty and completely filled channel (at $Da = 10^{-4}$), respectively.

5.3. Friction factor variation

Usage of the porous medium in a channel augments heat dissipation, but this comes at a price of the rise in pressure drop, increased need of pumping power. Furthermore, an increase in the number of porous blocks, with decreasing permeability can bring in unwanted pressure variation. Hence, it is utterly important to check for pressure losses to efficiently utilise the available energy with no or a little rise in pumping power. In Fig. 9 and Table 2, the calculated values of non-dimensional pressure drop (friction factor, $f = (H \times$

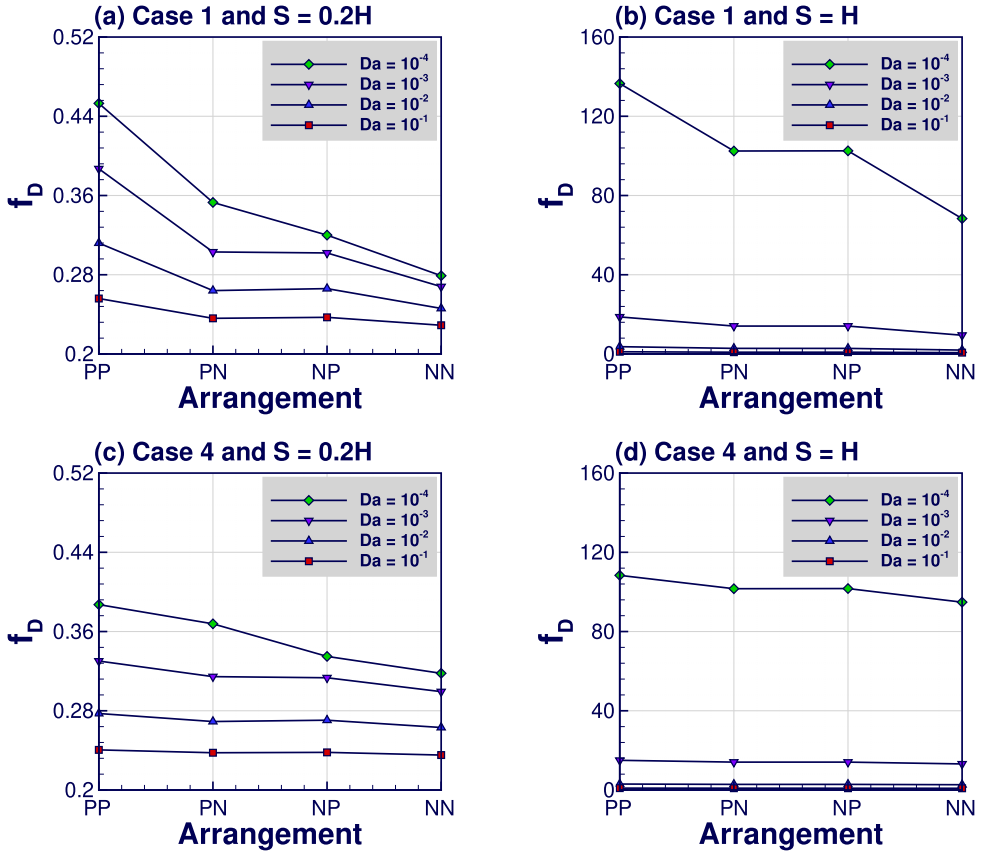

Fig. 9. Variation of friction factor (f_D) calculated by using pressure drop across the FPSC channel filled with blocks at various parameters.

$\Delta P)/(0.5\rho u^2 L))$ [17] are displayed. As *Da* increases, inertial and viscous resistances offered to the fluid flow decreases, and hence, f_D decreases without any exceptions. Also, it is clear that f_D is minimum for NN arrangement, followed by NP. The absence of the porous medium at the inlet of the FPSC channel is favourable of lower pressure drop, due to lesser resistance for the entering flow to develop quickly, resulting in lower pressure distribution. When *S* increases, friction factor tends to rise, as the fluid has a lesser area to escape without engaging with the porous medium. The increment in the number of blocks disrupts the formation of continuous hydrodynamics layer, discouraging viscous resistance and hence, a lower f_D value is reported for Case 4 in comparison to Case 1. In particular for NN arrangement, as seen in Table 2, very less f_D values are reported for $S = 0.2H$ and $0.4H$, while S ¿ $0.6H$ shows higher f_D.

5.4. Performance evaluation criteria (PEC)

After reviewing the increment in heat transfer along with the rise in the friction factor, it becomes vital to analyse the effectiveness of considered parameters to cast a balance between heat transfer augmentation and required efforts of pumping power. Resultingly, a Performance Evaluation Criterion (PEC) has been put forth as [17],

$$\mathrm{PEC} = \frac{\left(Nu_\alpha / Nu_{\alpha=0^o}\right)}{\left(f_{D\alpha} / f_{D\alpha=0^o}\right)^{1/3}}, \tag{11}$$

Details of PEC variation are shown in Figs. 10–12 for various parameters included in the study. It is clear that maximum thermal performance occurs at $Da = 10^{-1}$ for NN arrangement with $S = 0.2H$ when only one porous block exists *i.e*, Case 1. Further, after the NN arrangement, the PN arrangement shows higher PEC values at various parameters taken into account. Overall, NN and PN arrangement deliver better performance at higher Darcy number values, for a lesser number of porous blocks and minimum height *S*. Both, PP and NP arrangement for all cases, exhibit poor thermal performance, in spite of higher heat transfer rate with more number of porous blocks and higher height *S*. In conclusion, if the pressure drop is not a major concern, $S = 0.8H$ height of porous blocks provide maximum heat transfer augmentation. And if friction factor values are looked into, a lesser height of porous blocks with NN arrangement provides the highest PEC.

5.5. Darcy-Brinkman-Forchheimer extended model vs. Darcy-Brinkman model

In the present study, as the Reynolds number is fixed, it becomes necessary to check the validity of the inertia or the Forchheimer term of the extended Darcy-Brinkman-Forchheimer (D-B-F) model. Also, nowhere in the literature, such a comparison exists for the given combination of parameters. Table 3 details the distinction between D-B-F and D-B model for $S = 0.2H$ height of the porous block for various other parameters considered in the study. The percentage difference is calculated with respect to D-B-F model. Since, at this height, the resistance to the flow offered by the porous blocks is minimal, the validity of the porous media model is checked here. If the difference between the two models appears large at this height, it would be even higher for other *S* values as well. From the comparison, it is understood that at higher *Da*, D-B-F and D-B model provide almost the same results, while at lower *Da*

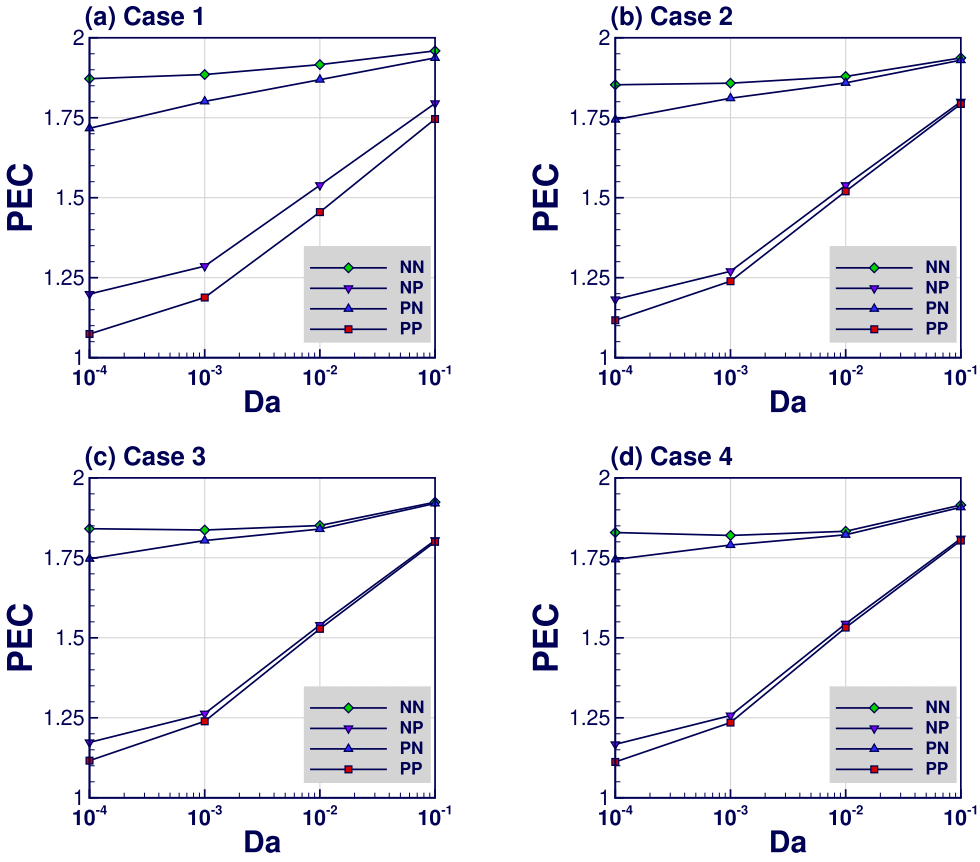

Fig. 10. Variation of Performance Evaluation Criteria (PEC) for different cases of porous blocks' number along with its arrangement at various Darcy number (Da) values. The height of porous blocks' is $S = 0.2H$.

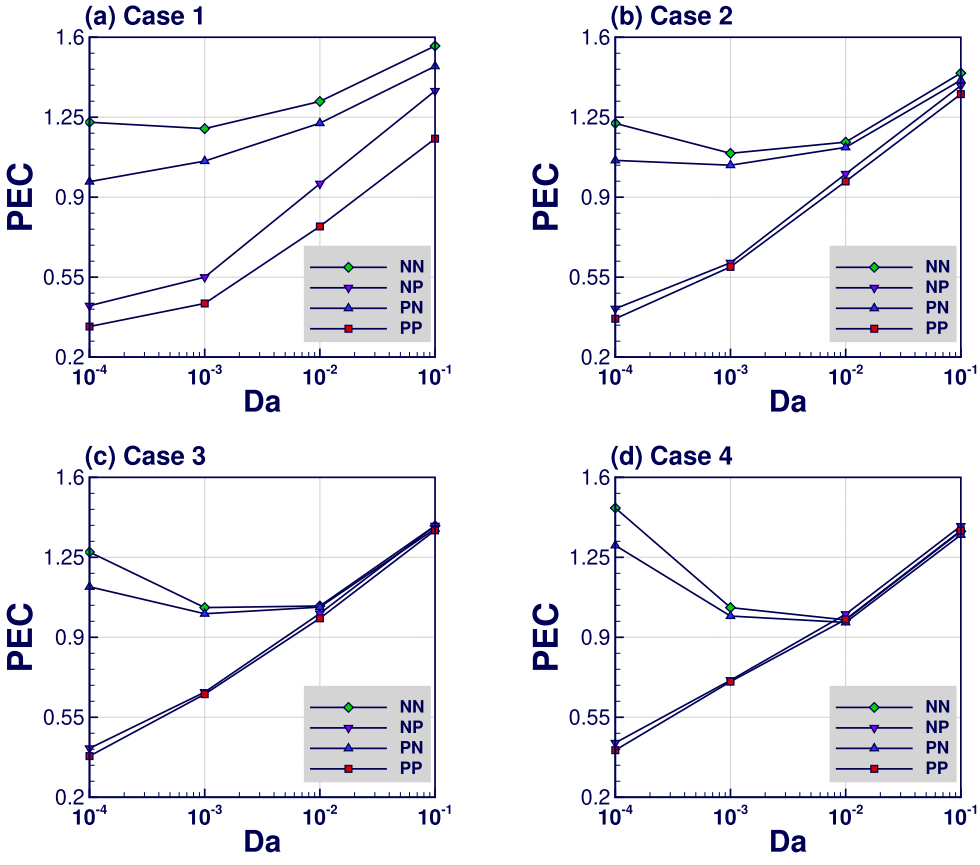

Fig. 11. Variation of Performance Evaluation Criteria (PEC) for different cases of porous blocks' number along with its arrangement at various Darcy number (Da) values. The height of porous blocks' is $S = 0.6H$.

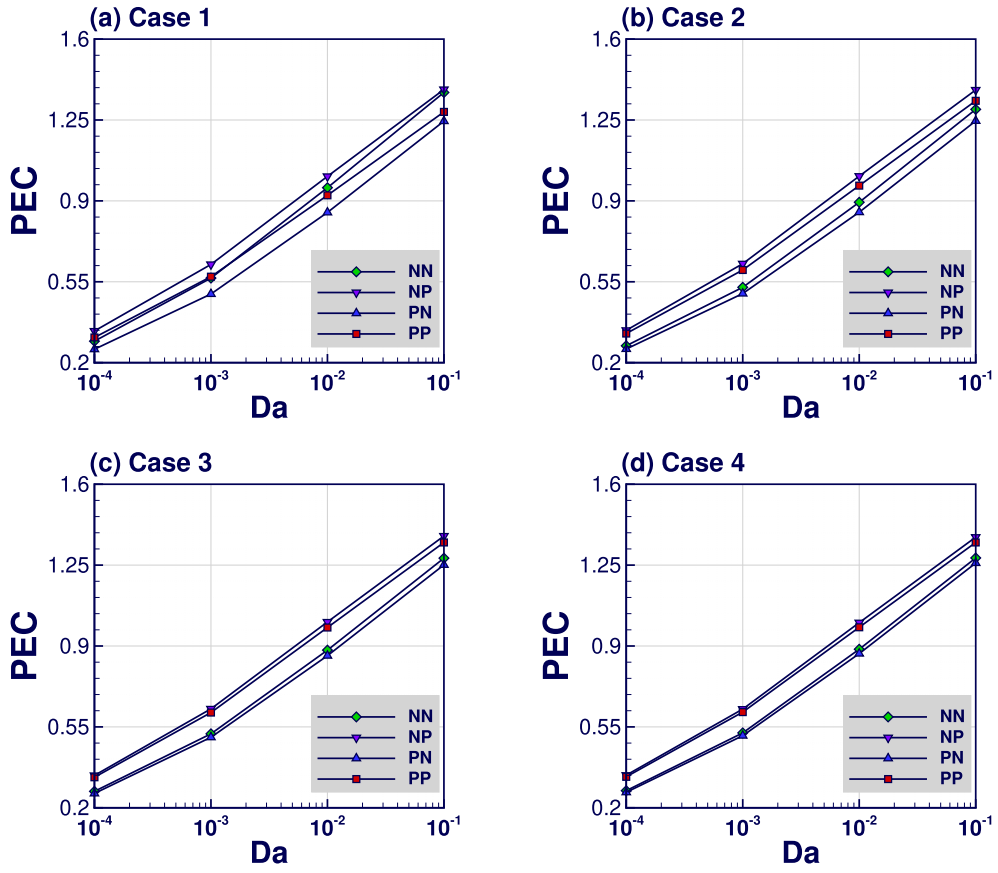

Fig. 12. Variation of Performance Evaluation Criteria (PEC) for different cases of porous blocks' number along with its arrangement at various Darcy number (*Da*) values. The height of porous blocks' is $S = H$.

Table 3
Comparison of (a) local Nusselt number (*Nu*) calculated at the top right end of the FPSC channel and (b) friction factor (f_D) for Darcy-Brinkman-Forchheimer extended model (D-B-F) and Darcy-Brinkman (D-B) model at porous block height of $S = 0.2H$ for different values of Darcy number *Da* and number of porous blocks.

		D-B-F				D-F				Percentage Difference (%)			
	Da	PP	PN	NP	NN	PP	PN	NP	NN	PP	PN	NP	NN
(a) *Nu*													
Case 2	10^{-4}	12.714	12.971	12.707	12.970	12.076	12.915	12.055	12.892	5.282	0.434	5.415	0.610
	10^{-1}	8.781	13.392	8.796	13.422	8.789	13.389	8.794	13.426	0.084	0.025	0.030	0.028
Case 4	10^{-4}	12.731	12.928	12.730	12.928	12.138	12.787	12.133	12.787	4.888	1.107	4.916	1.102
	10^{-1}	8.770	13.510	8.765	13.502	8.767	13.523	8.764	13.506	0.033	0.095	0.011	0.027
(b) f_D													
Case 2	10^{-4}	0.224	0.222	0.223	0.221	0.241	0.237	0.237	0.233	7.366	6.134	6.199	5.005
	10^{-1}	0.382	0.355	0.325	0.300	0.385	0.358	0.325	0.300	0.814	0.872	0.017	0.015
Case 4	10^{-4}	0.223	0.222	0.223	0.222	0.240	0.238	0.238	0.235	7.230	6.434	6.483	5.733
	10^{-1}	0.384	0.365	0.335	0.318	0.387	0.368	0.335	0.318	0.813	0.853	0.022	0.021

values the difference is serious. The maximum percentage difference is reported to be 5.415% and 7.336% for *Nu* and f_D, respectively. Hence, it is recommended that D-B-F model should be used for modelling the flow and heat transfer in the porous region of the FPSC channel filled with permeable blocks for obtaining results which can be considered legit.

6. Conclusions

An FPSC channel, filled with porous metal-foam blocks, is studied numerically and hydrodynamics and thermal performance are presented for domestic and industrial water heating applications. A generic code from the OpenFOAM® repository is modified, along with Darcy-Brinkman-Forchheimer extended model for realising porous medium, and the computations are carried out. The influence of placement, number, height, and arrangement of porous blocks on the FPSC performance is investigated. Numerical results suggest that the introduction of porous blocks results in higher heat dissipation from the absorber plate, in comparison to the insertion of a porous layer or filling of the channel with a porous medium. The heat transfer rate attains maximum value when the height of porous blocks lies between $S = 0.6H$ and H, particularly at $S = 0.8H$. Also, the augmentation in heat transfer is pronounced with the increasing number of permeable blocks. However, the penalty of higher values of friction factor has to be paid at this configuration, implying a significant demand of pumping power.

When the height of porous blocks decreases, thermal gradient near the wall increases, resulting in relatively higher heat transfer, but with little requirement for pumping power due to minor resistance being offered to fluid flow. Furthermore, better performance is predicted when the porous blocks are absent at the outlet, and preferably at the inlet. Perhaps best performance is anticipated for $S = 0.2H$ at NN configuration for higher values of permeability for single block placement. The information should be helpful for further experimental work on the present case, to check for the insertion of porous blocks for performance enhancement. A comment on the inclusion of the Forchheimer term in the current flow regime is also given. It is confirmed that using extended Darcy-Brinkman-Forchheimer model for modelling the porous channel would be proper. In future, Response Surface Methodology (RSM) can be applied for studying intricate details on the sensitivity of thermal buoyancy along with tampering with porous block properties.

Acknowledgment

One of the authors, S. Dhinakaran, gratefully acknowledges the fund received from Council of Scientific & Industrial Research (CSIR), Government of India, through a project grant (Project Reference No. 22(0642)/13/EMR-II) for carrying out this work.

References

[1] C.G. Granqvist, Transparent conductors as solar energy materials: a panoramic review, Sol. Energy Mater. Sol. Cell. 91 (17) (2007) 1529–1598.
[2] P. Vadász, Emerging Topics in Heat and Mass Transfer in Porous Media: from Bioengineering and Microelectronics to Nanotechnology, vol. 22, Springer Science & Business Media, 2008.
[3] P. Huang, K. Vafai, Analysis of forced convection enhancement in a channel using porous blocks, J. Thermophys. Heat Transf. 8 (3) (1994) 563–573.
[4] S. Chikh, A. Boumedien, K. Bouhadef, G. Lauriat, Analysis of fluid flow and heat transfer in a channel with intermittent heated porous blocks, Heat Mass Transf. 33 (5–6) (1998) 405–413.
[5] N. Guerroudj, H. Kahalerras, Mixed convection in a channel provided with heated porous blocks of various shapes, Energy Convers. Manag. 51 (3) (2010) 505–517.
[6] N. Guerroudj, H. Kahalerras, Mixed convection in an inclined channel with heated porous blocks, Int. J. Numer. Methods Heat Fluid Flow 22 (7) (2012) 839–861.
[7] C.-C. Chen, P.-C. Huang, Numerical study of heat transfer enhancement for a novel flat-plate solar water collector using metal-foam blocks, Int. J. Heat Mass Transf. 55 (23–24) (2012) 6734–6756.
[8] P.-C. Huang, C.-C. Chen, H.-Y. Hwang, Thermal enhancement in a flat-plate solar water collector by flow pulsation and metal-foam blocks, Int. J. Heat Mass Transf. 61 (2013) 696–720.
[9] C.-C. Chen, P.-C. Huang, H.-Y. Hwang, Enhanced forced convective cooling of heat sources by metal-foam porous layers, Int. J. Heat Mass Transf. 58 (1–2) (2013) 356–373.
[10] F. Lansing, V. Clarke, R. Reynolds, A high performance porous flat-plate solar collector, Energy 4 (4) (1979) 685–694.
[11] Z. Chen, M. Gu, D. Peng, Heat transfer performance analysis of a solar flat-plate collector with an integrated metal foam porous structure filled with paraffin, Appl. Therm. Eng. 30 (14–15) (2010) 1967–1973.
[12] S. Rashidi, M. Bovand, J. Esfahani, Heat transfer enhancement and pressure drop penalty in porous solar heat exchangers: a sensitivity analysis, Energy Convers. Manag. 103 (2015) 726–738.
[13] M. Bovand, S. Rashidi, J. Esfahani, Heat transfer enhancement and pressure drop penalty in porous solar heaters: numerical simulations, Sol. Energy 123 (2016) 145–159.
[14] H.J. Jouybari, S. Saedodin, A. Zamzamian, M.E. Nimvari, Experimental investigation of thermal performance and entropy generation of a flat-plate solar collector filled with porous media, Appl. Therm. Eng. 127 (2017) 1506–1517.
[15] H.J. Jouybari, S. Saedodin, A. Zamzamian, M.E. Nimvari, S. Wongwises, Effects of porous material and nanoparticles on the thermal performance of a flat plate solar collector: an experimental study, Renew. Energy 114 (2017) 1407–1418.
[16] H.J. Jouybari, S. Saedodin, S.A.H. Zamzamian, M.E. Nimvari, Analytical investigation of forced convection heat transfer in a flat-plate solar collector filled with a porous medium by considering radiation effect, J. Porous Media 21 (12) (2018) 1177–1195.
[17] S. Saedodin, S. Zamzamian, M.E. Nimvari, S. Wongwises, H.J. Jouybari, Performance evaluation of a flat-plate solar collector filled with porous metal foam: experimental and numerical analysis, Energy Convers. Manag. 153 (2017) 278–287.
[18] M. Ameri, M.S. Eshaghi, Exergy and thermal assessment of a Novel system utilizing flat plate collector with the application of nanofluid in porous media at a constant magnetic field, Thermal Sci. Eng. Progress 8 (2018) 223–235.
[19] S.A. Sakhaei, M.S. Valipour, Performance enhancement analysis of the flat plate collectors: a comprehensive review, Renew. Sustain. Energy Rev. 102 (2019) 186–204.
[20] S. Dhinakaran, J. Ponmozhi, Heat transfer from a permeable square cylinder to a flowing fluid, Energy Convers. Manag. 52 (5) (2011) 2170–2182.
[21] T.R. Vijaybabu, K. Anirudh, S. Dhinakaran, LBM simulation of unsteady flow and heat transfer from a diamond-shaped porous cylinder, Int. J. Heat Mass Transf. 120 (2018) 267–283.
[22] T.R. Vijaybabu, K. Anirudh, S. Dhinakaran, Lattice Boltzmann simulations of flow and heat transfer from a permeable triangular cylinder under the influence of aiding buoyancy, Int. J. Heat Mass Transf. 117 (2018) 799–817.
[23] T.R. Vijaybabu, K. Anirudh, S. Dhinakaran, Mixed convective heat transfer from a permeable square cylinder: a lattice Boltzmann analysis, Int. J. Heat Mass Transf. 115 (2017) 854–870.
[24] R. Khanal, C. Lei, Flow reversal effects on buoyancy induced air flow in a solar chimney, Sol. Energy 86 (9) (2012) 2783–2794.
[25] A. Hawwash, A.K.A. Rahman, S. Nada, S. Ookawara, Numerical investigation and experimental verification of performance enhancement of flat plate solar collector using nanofluids, Appl. Therm. Eng. 130 (2018) 363–374.
[26] H.G. Weller, G. Tabor, H. Jasak, C. Fureby, A tensorial approach to computational continuum mechanics using object-oriented techniques, Comput. Phys. 12 (6) (1998) 620–631.
[27] F.P. Kärrholm, Numerical Modelling of Diesel Spray Injection, Turbulence Interaction and Combustion, Chalmers University of Technology Gothenburg, 2008.
[28] P.J. Roache, Perspective: a method for uniform reporting of grid refinement studies, J. Fluids Eng. 116 (3) (1994) 405–413.
[29] T. Morosuk, Entropy generation in conduits filled with porous medium totally and partially, Int. J. Heat Mass Transf. 48 (12) (2005) 2548–2560.
[30] A. Mohamad, Heat transfer enhancements in heat exchangers fitted with porous media Part I: constant wall temperature, Int. J. Therm. Sci. 42 (4) (2003) 385–395.
[31] K. Anirudh, S. Dhinakaran, On the onset of vortex shedding past a two-dimensional porous square cylinder, J. Wind Eng. Ind. Aerodyn. 179 (2018) 200–214.
[32] K. Anirudh, S. Dhinakaran, Effects of Prandtl number on the forced convection heat transfer from a porous square cylinder, Int. J. Heat Mass Transf. 126 (2018) 1358–1375.